# State Estimation for Delayed Memristive Neural Networks With Multichannel Round-Robin Protocol and Multimodal Injection Attacks

Lijuan Zha, Jinzhao Miao, Jinliang Liu, *Member, IEEE*, Xiangpeng Xie, *Senior Member, IEEE*, and Engang Tian

***Abstract*—This article explores the state estimation problem of memristive neural networks (MNNs) with mixed delays subject to multichannel round-robin protocol (MRRP) and multimodal injection attacks (MIAs). MRRP allows for multichannel-enabled signal transmission between sensors and remote estimators, thereby significantly mitigating network congestion. Different types of attacks are supposed to be encountered during the sensor data transmission via network. Both the impacts of the MRRP and the attacks are reflected in modeling the addressed system. The purpose of this article is to design an estimator capable of constraining the estimation error within an ellipsoidal region in the presence of noise interference, mixed delays, MRRP, and MIAs. Using recursive matrix inequality (RMI) techniques, sufficient conditions are derived for achieving the desired performance and the expected state estimator gains are derived by minimizing the constrained ellipsoid region. Ultimately, the efficacy of the developed estimate strategy is demonstrated through numerical simulation.**

***Index Terms*—Memristive neural networks (MNNs), mixed delays, multichannel round-robin protocol (MRRP), multimodal injection attacks (MIAs), state estimation.**

## I. Introduction

FOR DECADES, memristive neural network (MNN) is an active area of research [1], [2], as it is widely applicable in domains, such as pattern recognition, digital image processing [3], and clustering analysis [4]. MNNs are artificial neural networks (NNs) that can capture historical information during learning. By enhancing the ability of the model to remember historical data, its predictive ability is strengthened. Unlike traditional NNs [5], [6], MNNs can update the current state based on input information and generate better output results [7]. MNNs have stronger spatiotemporal continuity, enabling the model to better handle time-series data and meet many requirements in practical applications.

The complexity and memory characteristics of MNNs pose a challenge in directly obtaining the neurons state of MNNs. To advance the development and deepen our understanding of the properties of MNNs in various domains, conducting extensive research on the state estimation problem of MNNs is imperative. Most existing analysis and estimation methods are developed based on traditional NNs, and their performance often falls short when dealing with MNNs that exhibit more complex dynamic behaviors. Consequently, the state estimation problem of MNNs, which has received relatively little attention at present, presents a highly valuable topic for further research.

In the realm of industrial applications, MNNs are commonly implemented using large-scale integrated circuits that include memristors. When implementing MNNs in actual scenarios, the limited information switching speed inevitably leads to time delays in the interaction among neurons [8], [9], [10]. In [11], a novel algebraic criteria has been introduced to assess the stability of synchronization in chaotic MNNs that have time-varying delays and external noise. An approach to stabilize second-order MNNs featuring mixed delays has been proposed in [12], using nonreduced-order techniques. Estimation methodology that accounts for delay distribution was presented in [13], specifically tailored for discrete-time MNNs that exhibit mixed delays. Time delays have been a consistently focal point in the field of MNNs and are recognized as a critical factor that affects estimation performance. Consequently, one of the primary focal points of this article is to develop the estimation strategy while considering the presence of mixed delays.

Due to the higher complexity of MNNs, the data quantity of measurement output can become rather large, leading to transmission conflicts and communication congestion issues

Manuscript received 29 October 2023; accepted 21 February 2024. Date of publication 12 March 2024; date of current version 17 May 2024. This work was supported in part by the National Natural Science Foundation of China under Grant 62273174, Grant 62373252, and Grant 61903182; in part by the Natural Science Foundation of Jiangsu Province of China under Grant BK20230063 and Grant BK20211290; and in part by the Qing Lan Project. This article was recommended by Associate Editor X. Li. *(Corresponding author: Jinliang Liu.)*

Lijuan Zha is with the School of Science, Nanjing Forestry University, Nanjing 210037, China, and also with the College of Information Engineering, Nanjing University of Finance and Economics, Nanjing 210023, China (e-mail: zhalijuan@vip.163.com).

Jinzhao Miao is with the College of Information Engineering, Nanjing University of Finance and Economics, Nanjing 210023, China (e-mail: miaojinzhao2022@163.com).

Jinliang Liu is with the School of Computer Science, Nanjing University of Information Science and Technology, Nanjing 210044, China (e-mail: liujinliang@vip.163.com).

Xiangpeng Xie is with the Institute of Advanced Technology, Nanjing University of Posts and Telecommunications, Nanjing 210023, China (e-mail: xiexiangpeng1953@163.com).

Engang Tian is with the School of Optical-Electrical and Computer Engineering, University of Shanghai for Science and Technology, Shanghai 200093, China (e-mail: tianengang@163.com).

Color versions of one or more figures in this article are available at https://doi.org/10.1109/TSMC.2024.3370221.

Digital Object Identifier 10.1109/TSMC.2024.3370221

in networks with limited transmission capacity [14], [15]. Industries have adopted communication scheduling protocols to address the challenges posed by limited network bandwidth. The employment of communication protocols and their impact on estimator performance has drawn significant attention [16]. Numerous researchers have identified communication protocols as a key factor for balancing estimation performance and network resources consumption [17], [18]. The impact of stochastic communication protocol (SCP) on the estimation of delayed genetic regulatory networks has been taken into consideration in [19]. In [20], the weighted try-once-discard (WTOD) protocol is introduced to alleviate network resource limitations in time-varying MNNs. In [21], the round-robin protocol (RRP) is utilized for scheduling signal transmission between variance-constrained filters with sensor resolutions and the sensor nodes. Among communication protocols, the RRP is extensively applied in practical engineering problems due to its simple implementation principle and equitable distribution of network communication resources. However, the existing RRP [21], [22], [23] occupies a single channel to transmit data, which means that only the signal of a single sensor node can be received by the remote estimator at each transmission moment. Although existing communication protocols can significantly reduce network conflicts, the decreased efficiency in updating output data leads to a decline in the performance of the estimator. To address this issue, this article introduces the multichannel RRP (MRRP), which enables signals from multiple nodes to be sent concurrently. By adjusting the number of occupied channel, the optimal estimator performance can be ensured while minimizing network burden issues. Hence, incorporating multichannel polling protocols into the design of estimators is a crucial focus of this research.

Recently, significant attention has been devoted to researching security issues pertaining to network attacks, including injection attacks [24], [25], denial-of-service attacks [26], [27], and deception attacks [28], [29], [30]. Attackers can disrupt the reliability and stability of NNs by confusing, altering, or deleting their input data, causing erratic output results. Injection attacks, which inject false signals into the system and lead to system malfunction, are particularly prevalent [31], [32]. An impulsive-based approach is proposed in [33] for achieving almost sure synchronization of NNs with deception attacks. The identification of injection attacks is addressed in [34], and a strategy is proposed for achieving efficient detection. In [35], a dynamic event-triggered control strategy is developed in MNNs to counter the threats to system security caused by network attacks. However, the current models for network attacks are based on a single attack strategy. In actual networks, malicious attackers often send multiple false signals to increase their chances of success [36]. The estimators designed solely for a single attack strategy may be vulnerable when facing injection attacks with multiple attack strategies [37]. Therefore, this article introduces the multimodal injection attacks (MIAs) that are capable of injecting multiple types of false signals. By doing so, we can enhance the robustness of the estimator against potentially devastating injection attacks.

By the Lyapunov function analysis method, a resilient estimation strategy is presented for MNNs incorporating stochastic delays in [38]. Based on Lyapunov functions, sufficient conditions are obtained in [13] for MNNs with fading measurements to ensure the error system remains bounded. However, when considering the scenarios involving communication protocols and network attacks, the existing estimate approaches are futile. Therefore, we introduce an analytical method that constrains the estimation error within an ellipsoidal range, which provides significant benefits in reducing the estimation error.

Drawing inspiration from the above discussions, this article primarily centers on devising a state estimator for MNNs with mixed delays, taking into consideration of the effects of MRRP and MIAs. The introduction of MRRP aims to schedule signal transmission to alleviate network congestion. The MIAs are also considered which can render the measurement data unreliable. The unique features of this article are summarized as follows.

1) A co-design method of the state and disturbance estimator is developed which is effective in handling the impact caused by mixed time delays, MPPR, and MIAs. The negative impacts of external disturbance can also be reduced with the designed disturbance estimator. By utilizing recursive matrix inequality (RMI), the estimation errors are constrained within designated ellipsoidal range and the optimal gain is obtained by minimizing the trace of constraint matrix.
2) Different from the results which avoid network conflicts and congestion by using WTOD protocol [20], SCP [19], and RRP [18], [21], the adopted MRRP in this article enables multiple transmission channels to have access to the network simultaneously instead of just one channel accessible to the network, which optimizes the usage of network resources and reduces network conflicts efficiently.
3) Compared with [4], [20], [31], [32], and [38], in which the state estimation problems were studied under the assumption that the transmission channel is secure or subject to single cyber-attacks, this work considers the scenarios of MIAs when designing the state estimator for MNNs, which surpasses the existing ones in terms of generality.

## II. Problem Formulation

### A. System Description

Consider MNNs with mixed delays in the following form:

$$\begin{cases} x(k+1) = A(x(k))x(k) + B(x(k))f(x(k)) \\ \qquad\qquad +D(x(k))f(x(k-\tau_1)) \\ \qquad\qquad +M(x(k))\sum_{t=1}^{\tau_2}\alpha_t g(x(k-t)) + G\omega(k) \\ y(k) = Cx(k) + H\omega(k) \end{cases} \tag{1}$$

where $x(k) = \mathrm{col}_n\{x_i(k)\}$ and $y(k) = \mathrm{col}_p\{y_i(k)\}$ are the neural state and the measurement output, respectively. $A(x(k)) = \mathrm{diag}_n\{a_i(x_i(k))\}$ is the self-feedback matrix with $|a_i(x_i(k))| < 1$. $B(x(k)) = (b_{ij}(x_i(k)))_{n\times n}$, $D(x(k)) = (d_{ij}(x_i(k)))_{n\times n}$, and $M(x(k)) = (m_{ij}(x_i(k)))_{n\times n}$ are connection weight matrices.

$C$, $G$, and $H$ are known matrices. $f(x(k)) = \text{col}_n\{f_i(x_i(k))\}$ and $g(x(k)) = \text{col}_n\{g_i(x_i(k))\}$ are the nonlinear neuron activation function (NAF). $\omega(k)$ denotes the external disturbance noise. The positive integers $\tau_1$ and $\tau_2$ are discrete and distributed delays, respectively. $x_0(k)(k = -\tau, -\tau+1, \ldots, 0)$ denotes initial state of $x(k)$ with $\tau = \max\{\tau_1, \tau_2\}$. $\alpha_t(t = 1, 2, \ldots, \tau_2)$ represents the connection weights.

The NAFs $f(\cdot)$ and $g(\cdot)$ satisfy the Lipschitz conditions

$$\|f(z_1) - f(z_2)\| \le \|\zeta_1(z_1 - z_2)\| \tag{2}$$

$$\|g(z_1) - f(z_2)\| \le \|\zeta_2(z_1 - z_2)\| \tag{3}$$

with $f(0) = g(0) = 0$, where $\zeta_1$ and $\zeta_2$ are known constant matrices.

Similar to the modeling approach used by [39] and [40], based on the characteristics of memristors, the state-dependent functions $a_i(x_i(\cdot))$, $b_{ij}(x_i(\cdot))$, $d_{ij}(x_i(\cdot))$, and $m_{ij}(x_i(\cdot))$ are defined as

$$a_i(x_i(\cdot)) = \begin{cases} \bar{a}_i, & |x_i(\cdot)| > \pi_i \\ \underline{a}_i, & |x_i(\cdot)| \le \pi_i \end{cases}$$

$$u_{ij}(x_i(\cdot)) = \begin{cases} \bar{u}_{ij}, & |x_i(\cdot)| > \pi_i \\ \underline{u}_{ij}, & |x_i(\cdot)| \le \pi_i \end{cases}$$

where $u$ denotes $b$, $d$, and $m$. $\pi_i$, $\bar{a}_i$, $\underline{a}_i$, $\bar{u}_{ij}$, and $\underline{u}_{ij}$ are known constants.

Denote

$$\begin{aligned}
&a_{i,\max} = \max\{\bar{a}_i, \underline{a}_i\}, \quad a_{i,\min} = \min\{\bar{a}_i, \underline{a}_i\} \\
&u_{ij,\max} = \max\{\bar{u}_{ij}, \underline{u}_{ij}\}, \quad u_{ij,\min} = \min\{\bar{u}_{ij}, \underline{u}_{ij}\} \\
&\hat{a}_i = \frac{a_{i,\max} + a_{i,\min}}{2}, \quad \check{a}_i = \frac{a_{i,\max} - a_{i,\min}}{2} \\
&\hat{u}_{ij} = \frac{u_{ij,\max} + u_{ij,\min}}{2}, \quad \check{u}_{ij} = \frac{u_{ij,\max} - u_{ij,\min}}{2} \\
&\gamma_{ij}^1 = 0\,(i \ne j), \quad \gamma_{ii}^1 = \sqrt{\frac{|\hat{a}_i - \check{a}_i|}{2}} \\
&\gamma_{ij}^2 = \sqrt{\frac{|\hat{b}_{ij} - \check{b}_{ij}|}{2}}, \quad \gamma_{ij}^3 = \sqrt{\frac{|\hat{d}_{ij} - \check{d}_{ij}|}{2}} \\
&\gamma_{ij}^4 = \sqrt{\frac{|\hat{m}_{ij} - \check{m}_{ij}|}{2}} \\
&\varpi_{ij}^l(x_i(k)) = \begin{cases} 1, & |x_i(\cdot)| > \pi_i \\ -1, & |x_i(\cdot)| \le \pi_i \end{cases}, \quad l = 1, 2, 3, 4.
\end{aligned}$$

Then, $A(x(k))$, $B(x(k))$, $D(x(k))$, and $M(x(k))$ are rewritten as $A(x(k)) = \bar{A} + \Delta A(k)$, $B(x(k)) = \bar{B} + \Delta B(k)$, $D(x(k)) = \bar{D} + \Delta D(k)$, and $M(x(k)) = \bar{M} + \Delta M(k)$, respectively, where

$$\begin{aligned}
&\bar{A} = \text{diag}_{1\le i\le n}\{\hat{a}_i\}, \quad \bar{B} = \left[\hat{b}_{ij}\right]_{n\times n} \\
&\bar{D} = \left[\hat{d}_{ij}\right]_{n\times n}, \quad \bar{M} = \left[\hat{m}_{ij}\right]_{n\times n} \\
&\Delta A(k) = E_1 Q_1(k) F_1, \quad \Delta B(k) = E_2 Q_2(k) F_2 \\
&\Delta D(k) = E_3 Q_3(k) F_3, \quad \Delta M(k) = E_4 Q_4(k) F_4 \\
&E_l = \left[\gamma_{11}^l \psi_1 \cdots \gamma_{1n}^l \psi_1 \cdots \gamma_{n1}^l \psi_n \cdots \gamma_{nn}^l \psi_n\right] \\
&Q_l(k) = \text{diag}\{\varpi_{11}^l(x_1(k)), \ldots, \varpi_{1n}^l(x_1(k)), \ldots \\
&\qquad\qquad \varpi_{n1}^l(x_n(k)), \ldots, \varpi_{nn}^l(x_n(k))\} \\
&F_l^T = \left[\gamma_{11}^l \psi_1 \cdots \gamma_{1n}^l \psi_n \cdots \gamma_{n1}^l \psi_1 \cdots \gamma_{nn}^l \psi_n\right].
\end{aligned}$$

$\psi_i$ is a standard basis vector with the $i$th entry equals to 1, and $Q_l^T(k) Q_l(k) \le I$.

Thus, MNNs (1) can be rewritten as

$$\begin{cases} x(k+1) = \big(\bar{A} + \Delta A(k)\big)x(k) + \big(\bar{B} + \Delta B(k)\big)f(x(k)) \\ \qquad\quad +\big(\bar{D} + \Delta D(k)\big)f(x(k - \tau_1)) \\ \qquad\quad +\big(\bar{M} + \Delta M(k)\big)\sum_{t=1}^{\tau_2} \alpha_t g(x(k-t)) + G\omega(k) \\ y(k) = Cx(k) + H\omega(k). \end{cases} \tag{4}$$

### B. Multichannel Round-Robin Protocol

MRRP is proposed for preventing congestion of constrained network caused by the massive signal transmission between sensors and remote estimators. In contrast to the conventional RRP which employs a single channel in [21], [22], and [23], this modified approach selects $s(1 \le s \le p)$ nodes for transmitting signals concurrently through $s$ assigned channels. The selected nodes set $S(k)$ is described as

$$S(k) = \big\{\big[s(k-1) + l\big]\%p + 1\big\}_{0\le l\le s-1} \tag{5}$$

where $p$ denotes the dimension of $y(k)$, and $l$ is an integer.

With the adoption of MRRP and the zero-order-hold (ZOH) strategy, the measurement output is updated by

$$\tilde{y}_i(k) = \begin{cases} y_i(k), & \text{if} i \in S(k) \\ \tilde{y}_i(k-1), & \text{otherwise} \end{cases} \tag{6}$$

where $\tilde{y}_i(k)$ denotes the signal that estimator receives without considering MIAs.

For presentation convenience, we define

$$\sigma_i(k) = \begin{cases} 1, & \text{if } i \in S(k) \\ 0, & \text{otherwise} \end{cases} \tag{7}$$

based on which, we can get

$$\tilde{y}(k) = \Phi_{\sigma(k)} y(k) + \big(I - \Phi_{\sigma(k)}\big)\tilde{y}(k-1) \tag{8}$$

where $\Phi_{\sigma(k)} = \text{diag}_{1\le i\le p}\{\sigma_i(k)\}$.

*Remark 1:* The existing RRP [21], [22], [23] assigns communication privileges to sensor nodes in a rotational manner, reducing the data throughput that the communication network needs to handle within a short time frame. This approach helps to minimize the occurrence of network conflicts and congestion, under which only one node can be arranged for signal transmission at each moment. However, the significant reduction in signal transmission volume also has a considerable adverse effect on the estimator performance. Network resources are often insufficient to support the transmission of data from all sensors but there is enough bandwidth to send a portion of the data. To fully utilize existing network resources, MRRP with adjustable channel usage has been introduced. It can specify the number of channels occupied when scheduling signals according to the specific network environment, balancing the conflicting relationship between limited network resources and estimator performance.

*Remark 2:* In order to better illustrate MRRP, a simple example is presented below. We assume that there are sensor nodes located in different regions, if two nodes will be selected from the three sensor nodes for transmission under MRRP,

that is, $p = 3$ and $s = 2$ in (5), the sensor nodes gain access to network will be in $S(k)$ at each moment, where

$$S(k) = \{[2(k-1)]\%3 + 1, [2(k-1)+1]\%3 + 1\}.$$

Then, we can obtain $S(1) = \{1, 2\}$, $S(2) = \{3, 1\}$, $S(3) = \{2, 3\}$, $S(4) = \{1, 2\}, \cdots$. Obviously, $S(k)$ is periodic sequence.

### C. Multimodal Injection Attacks

Communication network between sensors and remote estimators may be vulnerable to diverse malicious attacks launched by attackers aiming at the destruction of the information safety. In the following, we will consider MIAs with the characteristic of randomly sending multiple types of false data. The signal $\bar{y}(k)$ that estimator actually receives can be modeled as (9) in the presence of MIAs

$$\bar{y}(k) = \tilde{y}(k) + \mu(k)\sum_{j=1}^{q}\xi_j(k)\lambda_j(k) \tag{9}$$

where $\lambda_j(k)$ represents the misleading signal injected by the attacker. $\mu(k)$ and $\xi_j(k)$ are Bernoulli random variables with the expectation $\bar{\mu}$ and $\bar{\xi}_j$, respectively, which satisfy

$$\sum_{j=1}^{q}\xi_j(k) = 1, \quad \sum_{j=1}^{q}\bar{\xi}_j = 1.$$

Define

$$\xi(k) = \begin{bmatrix}\xi_1(k)I & \xi_2(k)I & \cdots & \xi_q(k)I\end{bmatrix}$$
$$\lambda(k) = \begin{bmatrix}\lambda_1^T(k) & \lambda_2^T(k) & \cdots & \lambda_q^T(k)\end{bmatrix}^T.$$

Taking into account actual cases of injection attacks, we postulate that $\lambda(k)$ satisfies

$$\lambda^T(k)\lambda(k) \le y^T(k)\vartheta^T\vartheta y(k) \tag{10}$$

where $\vartheta$ is a matrix with appropriate dimensions.

Combining (8) and (9) with the ZOH strategy, one has

$$\begin{aligned}\bar{y}(k) = {} & \Phi_{\sigma(k)}y(k) + \mu(k)\Phi_{\sigma(k)}\xi(k)\lambda(k) \\ & + \big(I - \Phi_{\sigma(k)}\big)\bar{y}(k-1).\end{aligned} \tag{11}$$

*Remark 3:* Bernoulli variable $\mu(k)$ in (11) is employed to indicate whether network attacks have occurred or not [41], [42]. When $\mu(k) = 1$, false data will be injected into the measurement output. Otherwise, there is no security threat, the estimator operates normally. Setting different values for $\bar{\mu}$ can change the frequency of attacks.

*Remark 4:* Compared with some single injection attacks in [24] and [34], the MIAs investigated in this article is more concealed due to the diversity of the attack means. In order to enhance the stealthiness of MIAs and avoid being detected, the attackers may launch different types of attack signals with different upper bound, which enhances the concealment of attack behavior. Therefore, it is meaning to address MIAs and ensure the systems work normally.

### D. Design of State Estimator and Disturbance Estimator

In view of the influences of the MRRP and MIAs, the following state estimator is devised for system (1):

$$\begin{aligned}\hat{x}(k+1) = {} & \bar{A}\hat{x}(k) + \bar{B}f\big(\hat{x}(k)\big) + \bar{D}f\big(\hat{x}(k-\tau_1)\big) \\ & + \bar{M}\sum_{t=1}^{\tau_2}\alpha_t g\big(\hat{x}(k-t)\big) \\ & + K(k)\big(\bar{y}(k) - C\hat{x}(k)\big) + G\hat{\omega}(k)\end{aligned} \tag{12}$$

where $\hat{x}(k)$ and $\hat{\omega}(k)$ are the estimation of $x(k)$ and $\omega(k)$, respectively. $K(k)$ is the gain matrix.

Similar to [43] and [44], for decreasing the impact of external disturbances on the estimation performance, devise a disturbance estimator as

$$\hat{\omega}(k+1) = \hat{\omega}(k) + L(k)\big(\bar{y}(k) - C\hat{x}(k)\big) \tag{13}$$

in which $L(k)$ is the gain matrix.

Define $e(k) = x(k) - \hat{x}(k)$ and $e_\omega(k) = \omega(k) - \hat{\omega}(k)$. From (4) and (12), the state estimation error $e(k)$ is derived as

$$\begin{aligned}e(k+1) = {} & \big(\bar{A} - K(k)C\big)e(k) + \big(\Delta A(k) + \tilde{K}(k)C\big)x(k) \\ & + \bar{B}\hat{f}(e(k)) + \Delta B(k)f(x(k)) \\ & + \bar{D}\hat{f}(e(k-\tau_1)) + \Delta D(k)f(x(k-\tau_1)) \\ & + \bar{M}\sum_{t=1}^{\tau_2}\alpha_t\hat{g}(e(k-t)) \\ & + \Delta M(k)\sum_{t=1}^{\tau_2}\alpha_t g(x(k-t)) - \tilde{K}(k)\bar{y}(k-1) \\ & - \mu(k)K(k)\Phi_{\sigma(k)}\xi(k)\lambda(k) + Ge_\omega(k) \\ & - K(k)\Phi_{\sigma(k)}H\omega(k)\end{aligned} \tag{14}$$

where

$$\begin{aligned}\tilde{K}(k) &= K(k)\big(I - \Phi_{\sigma(k)}\big) \\ \hat{f}(e(k)) &= f(x(k)) - f\big(\hat{x}(k)\big) \\ \hat{f}(e(k-\tau_1)) &= f(x(k-\tau_1)) - f\big(\hat{x}(k-\tau_1)\big) \\ \hat{g}(e(k-t)) &= g(x(k-t)) - g\big(\hat{x}(k-t)\big).\end{aligned}$$

From (9) and (13), we obtain the disturbance estimation error system as

$$\begin{aligned}e_\omega(k+1) = {} & e_\omega(k) + \Delta\omega(k) + \tilde{L}(k)Cx(k) - L(k)Ce(k) \\ & - \mu(k)L(K)\Phi_{\sigma(k)}\xi(k)\lambda(k) - \tilde{L}(k)\bar{y}(k-1)\end{aligned} \tag{15}$$

where

$$\tilde{L}(k) = L(k)\big(I - \Phi_{\sigma(k)}\big), \quad \Delta\omega(k) = \omega(k+1) - \omega(k).$$

Define $\eta(k) = \big[x^T(k)\ \bar{y}^T(k-1)\ e^T(k)\ e_\omega^T(k)\big]^T$, we can obtain

$$\begin{aligned}\eta(k+1) = {} & \mathcal{A}(k)\eta(k) + \mathcal{B}(k)\tilde{f}(\eta(k)) + \mathcal{D}(k)\tilde{f}(\eta(k-\tau_1)) \\ & + \mathcal{M}(k)\sum_{t=1}^{\tau_2}\alpha_t\tilde{g}(\eta(k-t)) + \mathcal{C}(k)\lambda(k) + \mathcal{G}(k)\omega(k)\end{aligned} \tag{16}$$

where

$$\mathcal{A}(k) = \tilde{\mathcal{A}}(k) + \Delta\mathcal{A}(k), \quad \mathcal{B}(k) = \tilde{\mathcal{B}}(k) + \Delta\mathcal{B}(k)$$

$$\mathcal{D}(k)=\tilde{\mathcal{D}}(k)+\Delta\mathcal{D}(k),\quad \mathcal{M}(k)=\tilde{\mathcal{M}}(k)+\Delta\mathcal{M}(k)$$
$$\tilde{f}(\eta(k))=\left[\hat{f}^T(e(k))\ f^T(x(k))\right]^T$$
$$\tilde{f}(\eta(k-\tau_1))=\left[\hat{f}^T(e(k-\tau_1))\ f^T(x(k-\tau_1))\right]^T$$
$$\tilde{g}(\eta(k-t))=\left[\hat{g}^T(e(k-t))\ g^T(x(k-t))\right]^T$$
$$\tilde{\mathcal{A}}(k)=\begin{bmatrix}\bar{A} & 0 & 0 & 0\\ \Phi_{\sigma(k)}C & I-\Phi_{\sigma(k)} & 0 & 0\\ \tilde{K}(k)C & -\tilde{K}(k) & \bar{A}-K(k)C & G\\ \tilde{L}(k)C & -\tilde{L}(k) & -L(k)C & I\end{bmatrix}$$
$$\Delta\mathcal{A}(k)=\begin{bmatrix}\Delta A(k) & 0 & 0 & 0\\ 0 & 0 & 0 & 0\\ \Delta A(k) & 0 & 0 & 0\\ 0 & 0 & 0 & 0\end{bmatrix}$$
$$\tilde{\mathcal{B}}(k)=\begin{bmatrix}0 & \bar{B}\\ 0 & 0\\ \bar{B} & 0\\ 0 & 0\end{bmatrix},\quad \Delta\mathcal{B}(k)=\begin{bmatrix}0 & \Delta B(k)\\ 0 & 0\\ 0 & \Delta B(k)\\ 0 & 0\end{bmatrix}$$
$$\tilde{\mathcal{D}}(k)=\begin{bmatrix}0 & \bar{D}\\ 0 & 0\\ \bar{D} & 0\\ 0 & 0\end{bmatrix},\quad \Delta\mathcal{D}(k)=\begin{bmatrix}0 & \Delta D(k)\\ 0 & 0\\ 0 & \Delta D(k)\\ 0 & 0\end{bmatrix}$$
$$\tilde{\mathcal{M}}(k)=\begin{bmatrix}0 & \bar{M}\\ 0 & 0\\ \bar{M} & 0\\ 0 & 0\end{bmatrix},\quad \Delta\mathcal{M}(k)=\begin{bmatrix}0 & \Delta M(k)\\ 0 & 0\\ 0 & \Delta M(k)\\ 0 & 0\end{bmatrix}$$
$$\mathcal{C}(k)=\begin{bmatrix}0\\ \mu(k)\Phi_{\sigma(k)}\xi(k)\\ -\mu(k)K(k)\Phi_{\sigma(k)}\xi(k)\\ -\mu(k)L(K)\Phi_{\sigma(k)}\xi(k)\end{bmatrix}$$
$$\mathcal{G}(k)=\begin{bmatrix}G\\ \Phi_{\sigma(k)}H\\ -K(k)\Phi_{\sigma(k)}H\\ J(k)-I\end{bmatrix}.$$

*Assumption 1 [44]:* For the external disturbances $\omega(k)$ and time-varying matrices $J(k)$, there exist known matrices $J_1$ and $J_2$ such that

$$\omega(k+1)=J(k)\omega(k),\quad J_1\le J(k)\le J_2. \tag{17}$$

*Assumption 2:* For known matrix $\tilde{P}(0)>0$, the initial state $x_0(k)(k=-\tau,-\tau+1,\ldots,0)$ satisfies

$$x_0^T(k)\tilde{P}^{-1}(0)x_0(k)\le 1. \tag{18}$$

*Assumption 3:* For known positive-definite matrix $W(k)$ and external disturbance $\omega(k)$, there exists

$$\omega^T(k)W^{-1}(k)\omega(k)\le 1. \tag{19}$$

This article focuses on proposing an estimator that can restrict the estimation error $e(k)$ and $e_\omega(k)$ within certain ellipsoidal regions. For augmented system (16) and positive matrix sequences $P(k)$, we hope to have sufficient conditions such that $\eta(k)$ satisfies the $P(k)$-dependent constraint as

$$\mathcal{P}(k)=\eta^T(k)P^{-1}(k)\eta(k)\le 1. \tag{20}$$

## III. Main Result

The objective of this section is to establish adequate prerequisites that ensure the fulfillment of $P(t)$-dependent constraint (20) by system (16). Afterward, an algorithm is presented to calculate $K(k)$ and $L(k)$ in the presence of MIAs and MRRP. We will begin by introducing a few lemmas that will assist in the ensuing derivation.

*Lemma 1 [20]:* The quadratic functions $Z_l(\varsigma)(\varsigma\in\mathbb{R}^r)$ are $Z_l(\varsigma)=\varsigma^TV_l\varsigma$, $(l=0,1,\ldots,\tilde{q})$ with $V_l^T=V_l$.

Then

$$Z_1(\varsigma)\le 0,\ldots,Z_{\tilde{q}}(\varsigma)\le 0\longrightarrow Z_0(\varsigma)\le 0 \tag{21}$$

holds if there exist $\beta_1>0,\ldots,\beta_{\tilde{q}}>0$ such that

$$V_0-\sum_{l=1}^{\tilde{q}}\beta_lV_l\le 0. \tag{22}$$

*Lemma 2 [45]:* For matrices $\Lambda=\Lambda^T$, $X$, $Y$ and $U^TU\le I$, then

$$\Lambda+XUY+(XUY)^T\le 0 \tag{23}$$

holds if there exists scalar $\varrho>0$ such that

$$\Lambda+\varrho XX^T+\varrho^{-1}Y^TY\le 0. \tag{24}$$

*Theorem 1:* Consider MNNs (1) and the estimator (12). The $P(t)$-dependent constraint is satisfied for the system (16) if there exist positive-definite matrices $P(k)$, $K(k)$, $L(k)$, scalars $\delta(k)$, $\epsilon_j(k)(j=1,2,3,4,5,6,7)$ such that

$$\begin{bmatrix}\Theta(k) & * & * & *\\ \hat{\Omega}(k) & -P(k+1) & * & *\\ \delta(k)\mathcal{E}^T & 0 & -\delta(k)I & *\\ \mathcal{F} & 0 & 0 & -\delta(k)I\end{bmatrix}\le 0 \tag{25}$$

where

$$\Theta(k)=\begin{bmatrix}-\tilde{\Xi}(k) & *\\ \tilde{\Omega}(k) & -P(k+1)\end{bmatrix}$$
$$\tilde{\Xi}(k)=\mathcal{I}_1+\sum_{j=1}^{7}\epsilon_j(k)\Xi_j(k)$$
$$\tilde{\Omega}(k)=\left[0\ \tilde{\mathcal{A}}(k)R(k)\ 0\ 0\ \tilde{\mathcal{B}}(k)\ \tilde{\mathcal{D}}(k)\ \tilde{\mathcal{M}}(k)\ \tilde{\mathcal{C}}(k)\ \tilde{\mathcal{G}}(k)\right]$$
$$\bar{\Omega}(k)=\begin{bmatrix}\underbrace{0\ldots0}_{7} & \bar{\mathcal{C}}(k) & 0\end{bmatrix},\quad \hat{\Omega}(k)=\left[\bar{\Omega}(k)\ 0\right]$$
$$\mathcal{I}_1=\mathrm{diag}\{1,\underbrace{0\ldots0}_{8}\},\quad \mathcal{I}_2=\begin{bmatrix}I & 0 & 0 & 0\end{bmatrix}$$
$$\mathcal{I}_3=\begin{bmatrix}0 & 0 & I & 0\end{bmatrix},\quad \Xi_1(k)=\mathrm{diag}\{-1,I,\underbrace{0\ldots0}_{7}\}$$
$$\Xi_2(k)=\mathrm{diag}\{-1,0,I,\underbrace{0\ldots0}_{6}\}$$
$$\Xi_3(k)=\mathrm{diag}\{0,-2R^T(k)\left(\mathcal{I}_3^T\zeta_1^T\zeta_1\mathcal{I}_3+\mathcal{I}_2^T\zeta_1^T\zeta_1\mathcal{I}_2\right)R(k)\ 0,0,I,0,0,0,0\}$$
$$\Xi_4(k)=\mathrm{diag}\{0,0,-2R^T(k-\tau_1)\left(\mathcal{I}_3^T\zeta_1^T\zeta_1\mathcal{I}_3+\mathcal{I}_2^T\zeta_1^T\zeta_1\mathcal{I}_2\right)R(k-\tau_1),0,0,I,0,0,0\}$$

$$\Xi_5(k) = \mathrm{diag}\{0, 0, 0, -\mathrm{diag}\{\tau_2\alpha_t^2(\mathcal{I}_3^T\zeta_2^T\zeta_2\mathcal{I}_3 + \mathcal{I}_2^T\zeta_2^T\zeta_2\mathcal{I}_2)\}_{1\le t\le\tau_2}, 0, 0, I, 0, 0\}$$
$$\Xi_6(k) = \mathrm{diag}\{0, -2R^T(k)\mathcal{I}_2^T C^T\vartheta^T\vartheta C\mathcal{I}_2 R(k), \underbrace{0\ldots0}_{5}, I, -2H^T\vartheta^T\vartheta H\}$$
$$\Xi_7(k) = \mathrm{diag}\{-1, \underbrace{0\ldots0}_{7}, W^{-1}(k)\}$$
$$\tilde{\mathcal{C}}(k) = \begin{bmatrix} 0 \\ \bar{\mu}\Phi_{\sigma(k)}\bar{\xi} \\ -\bar{\mu}K(k)\Phi_{\sigma(k)}\bar{\xi} \\ -\bar{\mu}L(K)\Phi_{\sigma(k)}\bar{\xi} \end{bmatrix}, \quad \bar{\mathcal{C}}(k) = \begin{bmatrix} 0 \\ \tilde{\mu}\Phi_{\sigma(k)}\tilde{\xi} \\ -\tilde{\mu}K(k)\Phi_{\sigma(k)}\tilde{\xi} \\ -\tilde{\mu}L(k)\Phi_{\sigma(k)}\tilde{\xi} \end{bmatrix}$$
$$\tilde{\mu} = \sqrt{\bar{\mu}(1-\bar{\mu})}, \quad \tilde{\xi}_j = \sqrt{\bar{\xi}_j(1-\bar{\xi}_j)}, (j = 1, 2, \ldots, q)$$
$$\bar{\xi} = \begin{bmatrix}\bar{\xi}_1 I & \bar{\xi}_2 I & \cdots & \bar{\xi}_q I\end{bmatrix}, \quad \tilde{\xi} = \begin{bmatrix}\tilde{\xi}_1 I & \tilde{\xi}_2 I & \cdots & \tilde{\xi}_q I\end{bmatrix}$$
$$\tilde{\mathcal{G}}(k) = \begin{bmatrix} G \\ \Phi_{\sigma(k)}H \\ -K(k)\Phi_{\sigma(k)}H \\ J_2 - I \end{bmatrix}, \quad \tilde{E}_l = \begin{bmatrix} E_l \\ 0 \\ E_l \\ 0 \end{bmatrix}, (l = 1, 2, 3, 4)$$
$$\mathcal{E}_l = \begin{bmatrix} \underbrace{0\ldots0}_{9} & \tilde{E}_l^T \end{bmatrix}^T, \quad \mathcal{E} = \begin{bmatrix}\mathcal{E}_1 & \mathcal{E}_2 & \mathcal{E}_3 & \mathcal{E}_4\end{bmatrix}$$
$$\tilde{F}_1 = \begin{bmatrix}F_1 & 0 & 0 & 0\end{bmatrix}, \quad \tilde{F}_\kappa = \begin{bmatrix}0 & F_\kappa\end{bmatrix}, (\kappa = 2, 3, 4)$$
$$\mathcal{F} = \begin{bmatrix} 0 & \tilde{F}_1 & 0 & 0 & 0 & 0 & 0 & 0 & 0 & 0 \\ 0 & 0 & 0 & 0 & \tilde{F}_2 & 0 & 0 & 0 & 0 & 0 \\ 0 & 0 & 0 & 0 & 0 & \tilde{F}_3 & 0 & 0 & 0 & 0 \\ 0 & 0 & 0 & 0 & 0 & 0 & \tilde{F}_4 & 0 & 0 & 0 \end{bmatrix}.$$

*Proof:* This theorem is demonstrated by employing mathematical induction. By applying Assumption 2, when $k = 0$

$$\mathbb{E}\{\mathcal{P}(0)\} = \mathbb{E}\left\{\eta^T(0)P^{-1}(0)\eta(0)\right\} \le 1. \tag{26}$$

Given that $\mathbb{E}\{\mathcal{P}(k)\} \le 1$, it is required to demonstrate the validity of $\mathbb{E}\{\mathcal{P}(k+1)\} \le 1$.

Applying the Cholesky decomposition to $P(k)$, we can have $P(k) = R(k)R^T(k)$, where $R(k)$ is a lower-triangular matrix. Referring to [46], we are aware that $\bar{\eta}(\iota)$ exists with $\|\bar{\eta}(\iota)\| \le 1$ such that $\eta(\iota) = R(\iota)\bar{\eta}(\iota)$ for $\iota \in \{0, 1, \ldots k\}$.

Define

$$\eta_{\tau_2}(k) = \begin{bmatrix}\eta^T(k-1) & \eta^T(k-2) & \cdots & \eta^T(k-\tau_2)\end{bmatrix}^T$$
$$\tilde{\eta}(k) = \Big[\, 1 \;\; \bar{\eta}^T(k) \;\; \bar{\eta}^T(k-\tau_1) \;\; \eta_{\tau_2}^T(k) \;\; \tilde{f}^T(\eta(k)) \;\; \tilde{f}^T(\eta(k-\tau_1)) \;\; \textstyle\sum_{t=1}^{\tau_2}\alpha_t\tilde{g}^T(\eta(k-t)) \;\; \lambda^T(k) \;\; \omega^T(k) \,\Big]^T$$
$$\Omega(k) = \begin{bmatrix} 0 & \mathcal{A}(k)R(k) & 0 & 0 & \mathcal{B}(k) & \mathcal{D}(k) \\ & & & & \mathcal{M}(k) & \mathcal{C}(k) \;\; \mathcal{G}(k) \end{bmatrix}$$

we have

$$\eta(k+1) = \Omega(k)\tilde{\eta}(k) \tag{27}$$

and thus

$$\mathbb{E}\{\mathcal{P}(k+1)\} - 1 = \mathbb{E}\left\{\tilde{\eta}^T(k)\left(\Omega^T(k)P^{-1}(k+1)\Omega(k) - \mathcal{I}_1\right)\tilde{\eta}(k)\right\}. \tag{28}$$

Considering $\|\bar{\eta}(\iota)\| \le 1(\iota \in \{0, 1, \ldots, k\})$, we obtain $\|\bar{\eta}(k)\|^2 \le 1$ and $\|\bar{\eta}(k-\tau_1)\|^2 \le 1$. Hence, one has

$$\tilde{\eta}^T(k)\Xi_1\tilde{\eta}(k) \le 0 \tag{29}$$
$$\tilde{\eta}^T(k)\Xi_2\tilde{\eta}(k) \le 0. \tag{30}$$

Noticing (2), we get

$$\tilde{f}^T(\eta(k))\tilde{f}(\eta(k)) \le e^T(k)\zeta_1^T\zeta_1 e(k) + x^T(k)\zeta_1^T\zeta_1 x(k) = \eta^T(k)\left(\mathcal{I}_3^T\zeta_1^T\zeta_1\mathcal{I}_3 + \mathcal{I}_2^T\zeta_1^T\zeta_1\mathcal{I}_2\right)\eta(k). \tag{31}$$

Based on (31), one obtains

$$\tilde{\eta}^T(k)\Xi_3\tilde{\eta}(k) \le 0 \tag{32}$$
$$\tilde{\eta}^T(k)\Xi_4\tilde{\eta}(k) \le 0. \tag{33}$$

Noting (3), we have

$$\left(\sum_{t=1}^{\tau_2}\alpha_t\tilde{g}(\eta(k-t))\right)^T\left(\sum_{t=1}^{\tau_2}\alpha_t\tilde{g}(\eta(k-t))\right) \le \tau_2\sum_{t=1}^{\tau_2}\alpha_t^2\tilde{g}^T(\eta(k-t))\tilde{g}(\eta(k-t)) \le \eta_{\tau_2}^T(k)\mathrm{diag}\{\tau_2\alpha_t^2\left(\mathcal{I}_3^T\zeta_2^T\zeta_2\mathcal{I}_3 + \mathcal{I}_2^T\zeta_2^T\zeta_2\mathcal{I}_2\right)\}_{1\le t\le\tau_2}\eta_{\tau_2}(k) \tag{34}$$

which can be rewritten as

$$\tilde{\eta}^T(k)\Xi_5\tilde{\eta}(k) \le 0. \tag{35}$$

In view of (10), one has

$$\mathbb{E}\{\lambda^T(k)\lambda(k)\} \le \left(Cx(k) + H\omega(k)\right)^T\vartheta^T\vartheta\left(Cx(k) + H\omega(k)\right) = 2\eta^T(k)\mathcal{I}_2^T C^T\vartheta^T\vartheta C\mathcal{I}_2\eta(k) + 2\omega^T(k)H^T\vartheta^T\vartheta H\omega(k). \tag{36}$$

It follows from (36) that:

$$\tilde{\eta}^T(k)\Xi_6(k)\tilde{\eta}(k) \le 0. \tag{37}$$

From Assumption 3, we get

$$\tilde{\eta}^T(k)\Xi_7(k)\tilde{\eta}(k) \le 0. \tag{38}$$

Using Lemma 1, one has

$$\mathbb{E}\left\{\Omega^T(k)P^{-1}(k+1)\Omega(k)\right\} - \mathcal{I}_1 - \sum_{j=1}^{7}\epsilon_j(k)\Xi_j(k) \le 0. \tag{39}$$

After calculating the expectations for $\mu(k)$ and $\xi(k)$, we can rewrite (39) with the Schur complement as

$$\begin{bmatrix} -\tilde{\Xi}(k) & * \\ \tilde{\Omega}(k) & -P(k+1) \end{bmatrix} + \bar{\Omega}^T(k)P^{-1}(k+1)\bar{\Omega}(k) + \mathbb{E}\left\{\mathcal{E}\mathcal{Q}(k)\mathcal{F} + (\mathcal{E}\mathcal{Q}(k)\mathcal{F})^T\right\} \le 0 \tag{40}$$

where

$$\mathcal{Q}(k) = \mathrm{diag}\{Q_1(k), Q_2(k), Q_3(k), Q_4(k)\}.$$

By applying Lemma 2 and Schur complement, it is easy to deduce (40) is ensured by (25). It follows from (25) that $\mathbb{E}\{\mathcal{P}(k+1)\} \le 1$. ■

**Algorithm 1** Calculating $K(k)$ and $L(k)$

Step 1. Set $k = 0$. The initial condition $P(0)$ and total sampling time $T$ are given.
Step 2. Calculate $R(k)$ based on $P(k) = R(k)R^T(k)$.
Step 3. Solving (41) under constraint (25). Then, we can obtain $K(k)$ and $L(k)$.
Step 4. Set $k = k + 1$. If $k > T$, go to Step 5, else, go to Step 2.
Step 5. Stop.

Next, we use convex optimization methods to minimize ellipsoid range constraint matrix $P(k+1)$ and provide an iterative algorithm for calculating the gain $K(k)$ and $L(k)$.

*Theorem 2:* Considering the system (16), the constraint matrix $P(k)$ is minimized if the parameters $K(t)$, $L(k)$, $\epsilon_j (j = 1, 2, \ldots, 7)$, and $\delta(k)$ are derived by solving the following optimization problem s.t. (25):

$$\min_{K(k),L(k),\epsilon_j,\delta(k)} \operatorname{tr}\{P(k+1)\}. \tag{41}$$

*Remark 5:* In Theorem 2, the state and disturbance estimator have been designed for MNNs subject to MRRP, MIAs, and disturbance noise. It can be seen from Theorem 2 and Algorithm 1 that the influences of these factors are reflected in the design process. The impacts of these factors are demonstrated by the simulation part.

*Remark 6:* The estimator gains can be derived by using Algorithm 1 and it will need to calculate the optimization problem on each iteration of the loop. The computational complexity of Algorithm 1 is dependent on the constraint condition LMI (25) in Theorem 1, the MRRP, the number of decision variables, and the dimensions of neural state $x(k)$ and the measurement output $y(k)$. The computational complexity of Algorithm 1 will increase if the dimensions of neural state and measurement output become higher and the number of decision variables and constraint conditions become larger.

## IV. Illustrative Example

In this section, an instance of simulation is presented to demonstrate the performance of the developed state estimator.

Consider MNNs (1) with parameters

$$a_1(x_1(\cdot)) = \begin{cases} 0.54, & |x_1(\cdot)| > 0.15 \\ 0.58, & |x_1(\cdot)| \le 0.15 \end{cases}$$
$$a_2(x_2(\cdot)) = \begin{cases} 0.64, & |x_2(\cdot)| > 0.15 \\ 0.82, & |x_2(\cdot)| \le 0.15 \end{cases}$$
$$b_{11}(x_1(\cdot)) = \begin{cases} -0.43, & |x_1(\cdot)| > 0.15 \\ 0.27, & |x_1(\cdot)| \le 0.15 \end{cases}$$
$$b_{12}(x_1(\cdot)) = \begin{cases} -0.35, & |x_1(\cdot)| > 0.15 \\ -0.28, & |x_1(\cdot)| \le 0.15 \end{cases}$$
$$b_{21}(x_2(\cdot)) = \begin{cases} 0.42, & |x_2(\cdot)| > 0.15 \\ -0.19, & |x_2(\cdot)| \le 0.15 \end{cases}$$
$$b_{22}(x_2(\cdot)) = \begin{cases} -0.31, & |x_2(\cdot)| > 0.15 \\ 0.34, & |x_2(\cdot)| \le 0.15 \end{cases}$$
$$d_{11}(x_1(\cdot)) = \begin{cases} 0.44, & |x_1(\cdot)| > 0.15 \\ 0.18, & |x_1(\cdot)| \le 0.15 \end{cases}$$
$$d_{12}(x_1(\cdot)) = \begin{cases} -0.37, & |x_1(\cdot)| > 0.15 \\ 0.23, & |x_1(\cdot)| \le 0.15 \end{cases}$$
$$d_{21}(x_2(\cdot)) = \begin{cases} 0.52, & |x_2(\cdot)| > 0.15 \\ -0.15, & |x_2(\cdot)| \le 0.15 \end{cases}$$
$$d_{22}(x_2(\cdot)) = \begin{cases} 0.61, & |x_2(\cdot)| > 0.15 \\ -0.16, & |x_2(\cdot)| \le 0.15 \end{cases}$$
$$m_{11}(x_1(\cdot)) = \begin{cases} 0.42, & |x_1(\cdot)| > 0.15 \\ 0.44, & |x_1(\cdot)| \le 0.15 \end{cases}$$
$$m_{12}(x_1(\cdot)) = \begin{cases} 0.18, & |x_1(\cdot)| > 0.15 \\ 0.15, & |x_1(\cdot)| \le 0.15 \end{cases}$$
$$m_{21}(x_2(\cdot)) = \begin{cases} 0.14, & |x_2(\cdot)| > 0.15 \\ 0.16, & |x_2(\cdot)| \le 0.15 \end{cases}$$
$$m_{22}(x_2(\cdot)) = \begin{cases} 0.62, & |x_2(\cdot)| > 0.15 \\ 0.67, & |x_2(\cdot)| \le 0.15 \end{cases}$$

$$C = \begin{bmatrix} 0.30 & 0.20 \\ 0.25 & 0.24 \\ 0.31 & 0.21 \end{bmatrix}, G = \begin{bmatrix} 0.12 & 0.21 \\ 0.24 & 0.16 \end{bmatrix}$$
$$H = \begin{bmatrix} 0.21 & 0.17 \\ 0.15 & 0.12 \\ 0.08 & 0.11 \end{bmatrix}.$$

The NAFs are set as

$$f(x(k)) = \begin{bmatrix} 0.22x_1(k) + 0.30\cos(2.78x_1(k)) \\ 0.25x_2(k) + 0.20\sin(3.86x_2(k)) \end{bmatrix}$$
$$g(x(k)) = \begin{bmatrix} 1.10x_1(k) - 3.12\sin(x_1(k)) \\ 2.21x_2(k) - 2.58\tan(x_2(k)) \end{bmatrix}$$

with the Lipschitz constant matrices

$$\zeta_1 = \begin{bmatrix} 1.85 & 0 \\ 0 & 1.02 \end{bmatrix}, \quad \zeta_2 = \begin{bmatrix} 4.22 & 0 \\ 0 & 4.79 \end{bmatrix}.$$

The random disturbance noise

$$\omega(k) = \begin{bmatrix} 0.12\sin(0.53k) + r_1(k) \\ 0.08\cos(0.45k) + r_2(k) \end{bmatrix}.$$

$r_1(k)$ and $r_2(k)$ are zero-mean random variables following a normal distribution with variances 0.02 and 0.03, respectively.

The scheduling policy of MRRP is introduced to prevent data collisions, under which each sensor node has equal opportunity to gain access to the network. Although there are three sensor nodes in this example, only two sensor nodes are permitted to transmitted their measurement outputs via the corresponding network channel at each time instant. The data transmission sequence is decided by the MRRP. Fig. 6 illustrates the selected nodes whose measurements will be transmitted under MRRP.

Set the occurring probability of MIAs $\bar{\mu} = 0.3$, the false signals are

$$\lambda_1(k) = \begin{bmatrix} 0.52\sin(k) & 0.23\sin(k) & 0.28\cos(k) \end{bmatrix}^T$$
$$\lambda_2(k) = \begin{bmatrix} 0.47\sin(k) & 0.22\sin(k) & 0.35\cos(k) \end{bmatrix}^T$$
$$\lambda_3(k) = \begin{bmatrix} 0.38\sin(k) & 0.17\sin(k) & 0.13\cos(k) \end{bmatrix}^T.$$

Let

$$\bar{\xi} = \begin{bmatrix} 0.3I & 0.3I & 0.4I \end{bmatrix}, \quad \vartheta = \begin{bmatrix} 1.37 & 0 & 0 \\ 0 & 0.62 & 0 \\ 0 & 0 & 0.76 \end{bmatrix}.$$

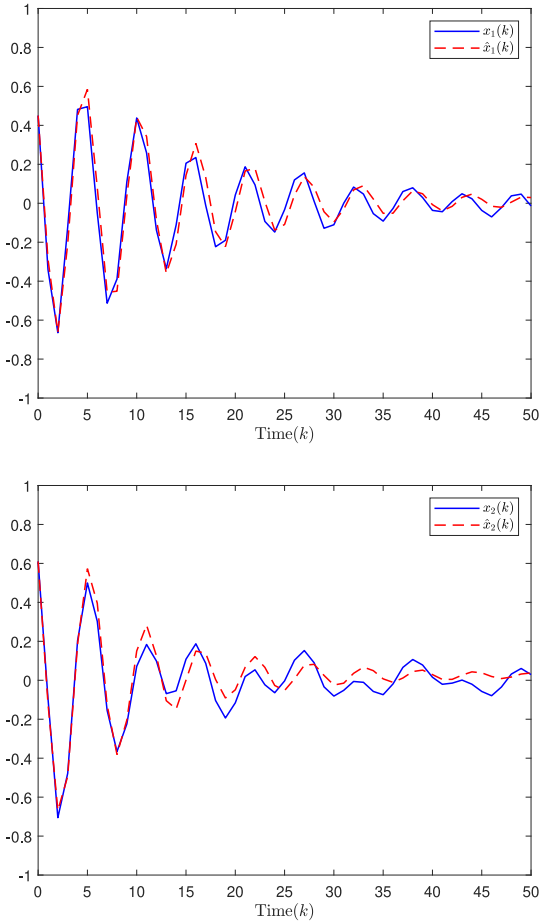


Fig. 1. $x(k)$ and its estimation $\hat{x}(k)$ under $\tau_1$ and $\tau_2$.

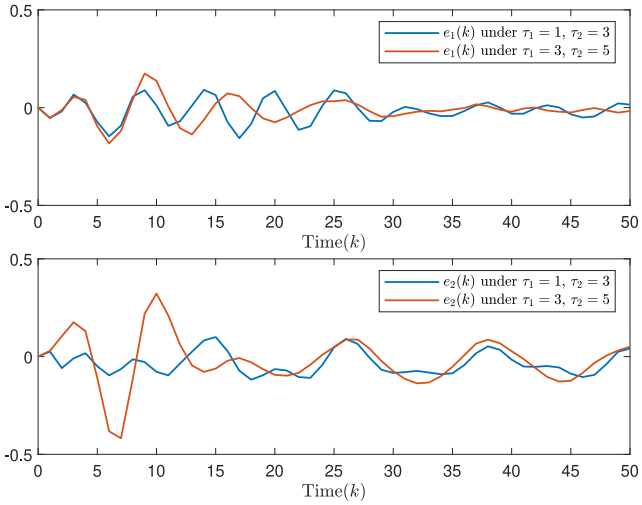


Fig. 2. State estimation error $e(k)$ under different delays.

The initial states are

$$x_0(k) = \begin{bmatrix}0.45 & 0.61\end{bmatrix}^T, (k = -\tau, -\tau+1, \ldots, 0)$$

and $P(0) = 0.85I$.

Through utilizing the MATLAB YALMIP 4.0 toolbox, we have solved the optimization problem (41) and the simulation results are demonstrated in Figs. 1–8. For given $\tau_1 = 1$, $\tau_2 = 3$, $\alpha_1 = 0.6$, $\alpha_2 = 0.3$, $\alpha_3 = 0.1$, the system state $x(k)$ and its estimate $\hat{x}(k)$ are displayed in Fig. 1, which shows that the designed estimator can approximate the system state. The influences of the time delays are examined in Fig. 2, which depicts the estimation errors for given different time delays. From Fig. 2, we can see higher delays have a certain adverse effect on the performance of the estimator.

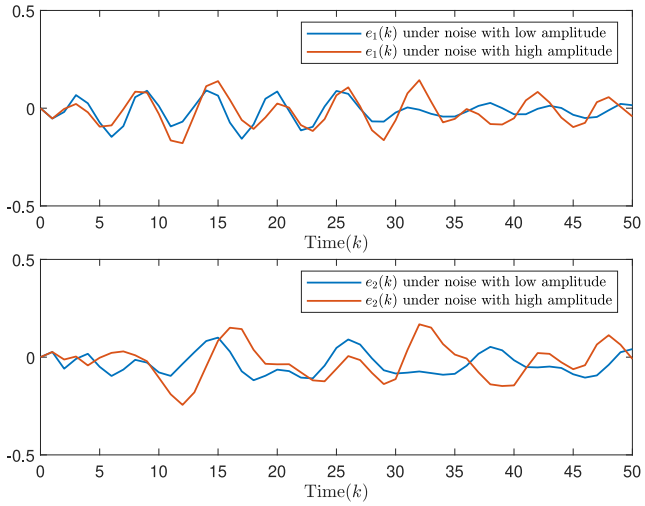


Fig. 3. $e(k)$ under different noise.

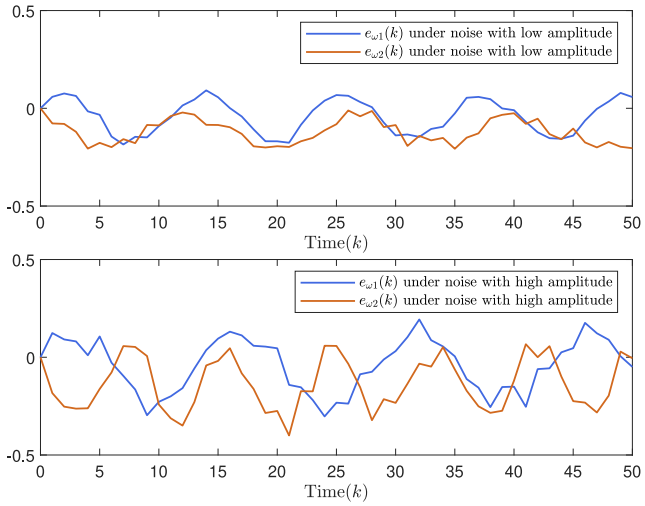


Fig. 4. $e_\omega(k)$ under different noise.

The following presented simulation results are under delays $\tau_1 = 1$ and $\tau_2 = 3$.

To examine the impact of random disturbance noise on estimation performance, a comparison is provided in Figs. 3 and 4. Set the disturbance noise with high amplitude as follows:

$$\omega(k) = \begin{bmatrix}0.23\sin(0.43k) + r_3(k) \\ 0.21\cos(0.73k) + r_4(k)\end{bmatrix}.$$

$r_3(k)$ and $r_4(k)$ are zero-mean random variables following a normal distribution with variances 0.06 and 0.07, respectively.

Fig. 3 demonstrates the state estimation error $e(k)$ under different noise. Fig. 4 displays the disturbance estimation error $e_\omega(k)$ under different noise. From Figs. 3 and 4, it can be

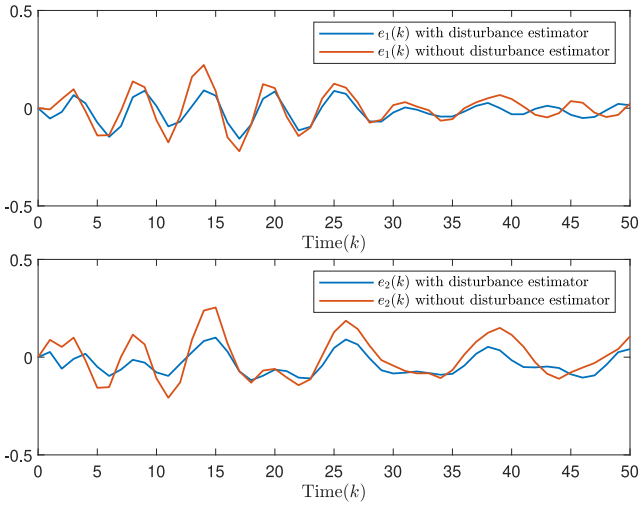


Fig. 5. $e(k)$ with and without disturbance estimator.

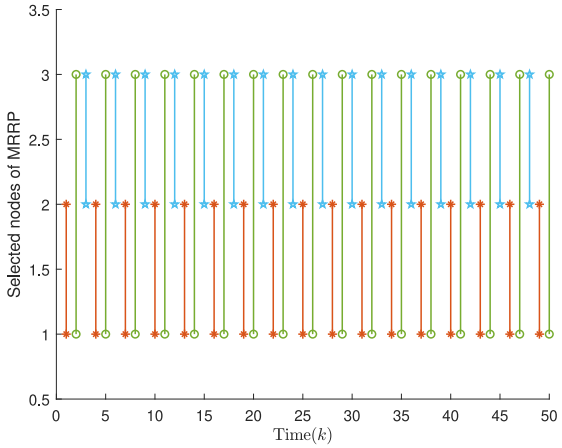


Fig. 6. Selected nodes under MRRP.

observed that the stronger disturbance noise may cause a slight increase in estimation errors $e(k)$ and $e_{\omega(k)}$.

Fig. 5 illustrates the $e(k)$ without and with the disturbance estimator, which shows the disturbance estimator is capable of estimating the external noise. By employing the disturbance estimator, the adverse impact of unknown disturbance noise on the accuracy of state estimation is further reduced. The average state estimation error decreases a bit.

Fig. 7 illustrates the instants of MIAs with low amplitude and the selected attack strategy $\lambda_j(k)$. To assess the impact of different MIAs on estimation performance, set the false signal of MIAs with high amplitude as follows:

$$\lambda_1(k) = \begin{bmatrix} 1.02\sin(k) & 0.73\sin(k) & 0.78\cos(k) \end{bmatrix}^T$$
$$\lambda_2(k) = \begin{bmatrix} 0.97\sin(k) & 0.72\sin(k) & 0.85\cos(k) \end{bmatrix}^T$$
$$\lambda_3(k) = \begin{bmatrix} 0.88\sin(k) & 0.67\sin(k) & 0.63\cos(k) \end{bmatrix}^T.$$

Fig. 8 displays the state estimation error $e(k)$ without attacks and under different attacks, which illustrate that the estimation error increases under MIAs. Furthermore, an escalation in the amplitude of MIAs also leads to a further

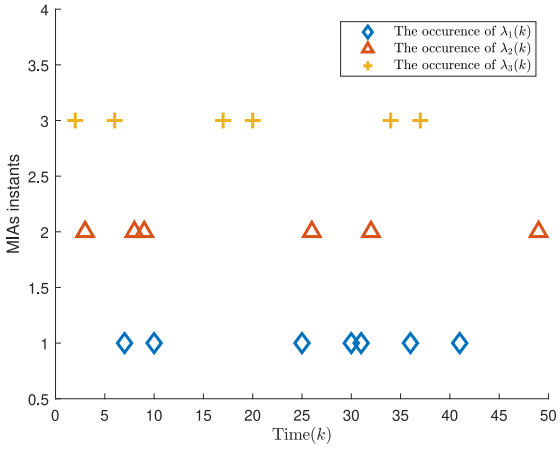


Fig. 7. Instants of MIAs occurrence.

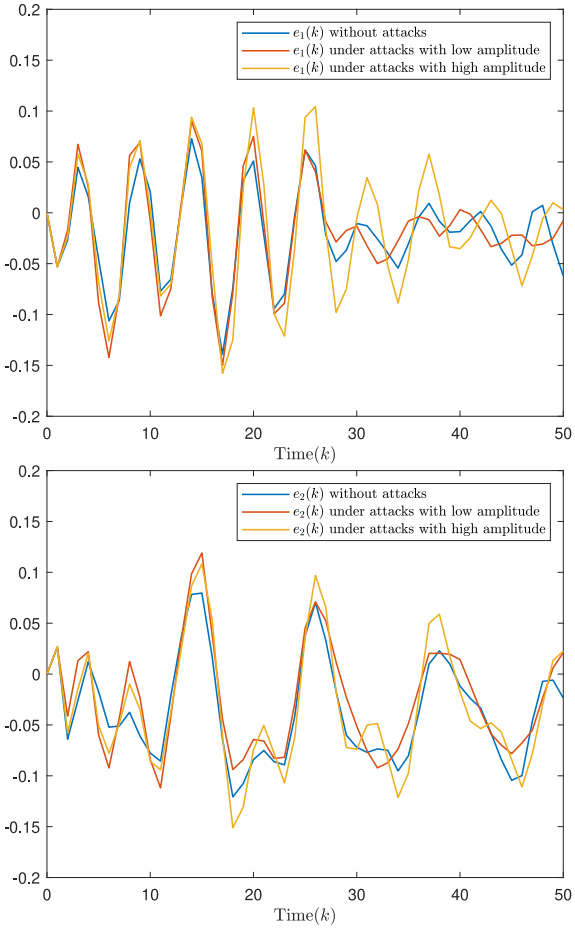


Fig. 8. $e(k)$ without attacks and under different attacks.

amplification of $e(k)$. From the simulation outcomes mentioned above, we can see the designed state estimation strategy works well under the MRRP and the MIAs.

## V. Conclusion

This article has explored the state estimation for MNNs with mixed delays, MRRP, and MIAs. MRRP is implemented to arrange a plurality of sensor nodes concurrently transmit their signals, with the aim of easing network congestion

and decreasing network load. The proposed MIAs with different attack strategies are addressed which is practical for actual scenarios. Through the application of RMI technique, sufficient conditions to limit the estimation error within a specified ellipsoidal range are established. The estimator gains are obtained by solving the optimization problem presented in Theorem 2, and their effectiveness is confirmed through simulation results. In addition, sliding-mode observers design for MNNs is an interesting problem. Moving forward, we will investigate the sliding-mode observer and external disturbance observer design for MNNs.

## REFERENCES


[1] D. Liu and D. Ye, "Exponential stabilization of delayed inertial memristive neural networks via aperiodically intermittent control strategy," *IEEE Trans. Syst., Man, Cybern., Syst.*, vol. 52, no. 1, pp. 448–458, Jan. 2022.

[2] Y. Sheng, T. Huang, and Z. Zeng, "Exponential stabilization of fuzzy memristive neural networks with multiple time delays via intermittent control," *IEEE Trans. Syst., Man, Cybern., Syst.*, vol. 52, no. 5, pp. 3092–3101, May 2022.

[3] M. Yuan, W. Wang, Z. Wang, X. Luo, and J. Kurths, "Exponential Synchronization of delayed memristor-based uncertain complex-valued neural networks for image protection," *IEEE Trans. Neural Netw. Learn. Syst.*, vol. 32, no. 1, pp. 151–165, Jan. 2021.

[4] H. Liu, Z. Wang, and L. Ma, *Stability Analysis and State Estimation of Memristive Neural Networks*. Boca Raton, FL, USA: CRC Press, 2021.

[5] S. Kundu, M. Nazemi, M. Pedram, K. M. Chugg, and P. A. Beerel, "Pre-defined sparsity for low-complexity convolutional neural networks," *IEEE Trans. Comput.*, vol. 69, no. 7, pp. 1045–1058, Jul. 2020.

[6] S. Dey, K.-W. Huang, P. A. Beerel, and K. M. Chugg, "Pre-defined sparse neural networks with hardware acceleration," *IEEE J. Emerg. Sel. Topics Circuits Syst.*, vol. 9, no. 2, pp. 332–345, Jun. 2019.

[7] W. Yao, C. Wang, Y. Sun, and C. Zhou, "Robust multimode function synchronization of memristive neural networks with parameter perturbations and time-varying delays," *IEEE Trans. Syst., Man, Cybern., Syst.*, vol. 52, no. 1, pp. 260–274, Jan. 2022.

[8] Z. Zhang, X. Liu, D. Zhou, C. Lin, J. Chen, and H. Wang, "Finite-time stabilizability and instabilizability for complex-valued memristive neural networks with time delays," *IEEE Trans. Syst., Man, Cybern., Syst.*, vol. 48, no. 12, pp. 2371–2382, Dec. 2018.

[9] L. Wang, Z. Zeng, and M.-F. Ge, "A disturbance rejection framework for finite-time and fixed-time Stabilization of delayed memristive neural networks," *IEEE Trans. Syst., Man, Cybern., Syst.*, vol. 51, no. 2, pp. 905–915, Feb. 2021.

[10] H. Liu, Z. Wang, B. Shen, and X. Liu, "Event-triggered $H_\infty$ state estimation for delayed stochastic Memristive neural networks with missing measurements: The discrete time case," *IEEE Trans. Neural Netw. Learn. Syst.*, vol. 29, no. 8, pp. 3726–3737, Aug. 2018.

[11] G. Zhang and Y. Shen, "New algebraic criteria for synchronization stability of chaotic memristive neural networks with time-varying delays," *IEEE Trans. Neural Netw. Learn. Syst.*, vol. 24, no. 10, pp. 1701–1707, Oct. 2013.

[12] G. Zhang and Z. Zeng, "Stabilization of second-order memristive neural networks with mixed time delays via nonreduced order," *IEEE Trans. Neural Netw. Learn. Syst.*, vol. 31, no. 2, pp. 700–706, Feb. 2020.

[13] H. Liu, Z. Wang, B. Shen, and H. Dong, "Delay-distribution-dependent $H_\infty$ state estimation for discrete-time memristive neural networks with mixed time-delays and fading measurements," *IEEE Trans. Cybern.*, vol. 50, no. 2, pp. 440–451, Feb. 2020.

[14] Y. Luo, Z. Wang, Y. Chen, and X. Yi, "$H_\infty$ state estimation for coupled stochastic complex networks with periodical communication protocol and intermittent nonlinearity switching," *IEEE Trans. Netw. Sci. Eng.*, vol. 8, no. 2, pp. 1414–1425, Apr.–Jun. 2021.

[15] Y. Luo, Z. Wang, W. Sheng, and D. Yue, "State estimation for discrete time-delayed impulsive neural networks under communication constraints: A delay-range-dependent approach," *IEEE Trans. Neural Netw. Learn. Syst.*, vol. 34, no. 3, pp. 1489–1501, Mar. 2023.

[16] F. Wang, Z. Wang, J. Liang, and X. Liu, "Resilient filtering for linear time-varying repetitive processes under uniform quantizations and round-robin protocols," *IEEE Trans. Circuits Syst. I, Reg. Papers*, vol. 65, no. 9, pp. 2992–3004, Sep. 2018.

[17] J. Liu, E. Gong, L. Zha, E. Tian, and X. Xie, "Observer-based security fuzzy control for nonlinear networked systems under weighted try-once-discard protocol," *IEEE Trans. Fuzzy Syst.*, vol. 31, no. 11, pp. 3853–3865, Nov. 2023.

[18] J. Liu, E. Gong, L. Zha, X. Xie, and E. Tian, "Outlier-resistant recursive security filtering for multirate networked systems under fading measurements and round-robin protocol," *IEEE Trans. Control Netw. Syst.*, vol. 10, no. 4, pp. 1962–1974, Dec. 2023.

[19] X. Wan, Z. Wang, Q.-L. Han, and M. Wu, "Finite-time $H_\infty$ state estimation for discrete time-delayed genetic regulatory networks under stochastic communication protocols," *IEEE Trans. Circuits Syst. I, Reg. Papers*, vol. 65, no. 10, pp. 3481–3491, Oct. 2018.

[20] H. Liu, Z. Wang, W. Fei, and H. Dong, "On state estimation for discrete time-delayed memristive neural networks under the WTOD protocol: A resilient set-membership approach," *IEEE Trans. Syst., Man, Cybern., Syst.*, vol. 52, no. 4, pp. 2145–2155, Apr. 2022.

[21] H. Geng, Z. Wang, J. Hu, Q.-L. Han, and Y. Cheng, "Variance-constrained filter design with sensor resolution under round-robin communication protocol: An outlier-resistant mechanism," *IEEE Trans. Syst., Man, Cybern., Syst.*, vol. 53, no. 6, pp. 3762–3773, Jun. 2023.

[22] Z. Zhang, Y. Niu, and H. R. Karimi, "Sliding mode control of interval type-2 fuzzy systems under round-robin scheduling protocol," *IEEE Trans. Syst., Man, Cybern., Syst.*, vol. 51, no. 12, pp. 7602–7612, Dec. 2021.

[23] L. Zou, Z. Wang, Q.-L. Han, and D. Yue, "Tracking control under round-robin scheduling: Handling impulsive transmission outliers," *IEEE Trans. Cybern.*, vol. 53, no. 4, pp. 2288–2300, Apr. 2023.

[24] W. Qi, Y. Hou, G. Zong, and C. K. Ahn, "Finite-time event-triggered control for semi-Markovian switching cyber-physical systems with FDI attacks and applications," *IEEE Trans. Circuits Syst. I, Reg. Papers*, vol. 68, no. 6, pp. 2665–2674, Jun. 2021.

[25] L. Zha, R. Liao, J. Liu, X. Xie, E. Tian, and J. Cao, "Dynamic event-triggered output feedback control for networked systems subject to multiple cyber attacks," *IEEE Trans. Cybern.*, vol. 52, no. 12, pp. 13800–13808, Dec. 2022.

[26] J. Xie, S. Zhu, and D. Zhang, "Asynchronous-switching-based distributed interval filtering for positive Markov jump linear systems under denial-of-service attack," *IEEE Trans. Syst., Man, Cybern.: Syst.*, vol. 53, no. 3, pp. 2004–2009, Mar. 2023.

[27] X. Li and J. Wang, "Resilient consensus for networked lagrangian systems with disturbances and DoS attacks," *IEEE Trans. Syst., Man, Cybern., Syst.*, vol. 53, no. 3, pp. 1644–1655, Mar. 2023.

[28] J. Cheng, Y. Wu, Z.-G. Wu, and H. Yan, "Nonstationary filtering for fuzzy Markov switching affine systems with quantization effects and deception attacks," *IEEE Trans. Syst., Man, Cybern., Syst.*, vol. 52, no. 10, pp. 6545–6554, Oct. 2022.

[29] D. Ding, Z. Wang, Q.-L. Han, and G. Wei, "Security control for discrete-time stochastic nonlinear systems subject to deception attacks," *IEEE Trans. Syst., Man, Cybern., Syst.*, vol. 48, no. 5, pp. 779–789, May 2018.

[30] Y. Luo, Z. Wang, J. Hu, H. Dong, and D. Yue, "Security-guaranteed fuzzy networked state estimation for 2-D systems with multiple sensor arrays subject to deception attacks," *IEEE Trans. Fuzzy Syst.*, vol. 31, no. 10, pp. 3624–3638, Oct. 2023.

[31] J. Liu, E. Gong, L. Zha, E. Tian, and X. Xie, "Interval type-2 fuzzy-model-based filtering for nonlinear systems with event-triggering weighted try-once-discard protocol and cyberattacks," *IEEE Trans. Fuzzy Syst.*, vol. 32, no. 3, pp. 721–732, Mar. 2024.

[32] E. Tian, H. Chen, C. Wang, and L. Wang, "Security-ensured state of charge estimation of lithium-ion batteries subject to malicious attacks," *IEEE Trans. Smart Grid*, vol. 14, no. 3, pp. 2250–2261, May 2023.

[33] S. Dong, H. Zhu, S. Zhong, K. Shi, and J. Lu, "Impulsive-based almost surely synchronization for neural network systems subject to deception attacks," *IEEE Trans. Neural Netw. Learn. Syst.*, vol. 34, no. 5, pp. 2298–2307, May 2023.

[34] Y. Wang, Z. Zhang, J. Ma, and Q. Jin, "KFRNN: An effective false data injection attack detection in smart grid based on Kalman filter and recurrent neural network," *IEEE Internet Things J.*, vol. 9, no. 9, pp. 6893–6904, May 2022.

[35] X. Wang, J. H. Park, Z. Liu, and H. Yang, "Dynamic event-triggered control for GSES of memristive neural networks under multiple cyber-attacks," *IEEE Trans. Neural Netw. Learn. Syst.*, early access, Nov. 7, 2022, doi: 10.1109/TNNLS.2022.3217461.

[36] F. Qu, E. Tian, and X. Zhao, "Chance-constrained $H_\infty$ state estimation for recursive neural networks under deception attacks and energy constraints: The finite-horizon case," *IEEE Trans. Neural Netw. Learn. Syst.*, vol. 34, no. 9, pp. 6492–6503, Sep. 2023.

[37] X. Wang, E. Tian, B. Wei, and J. Liu, "Novel attack-defense framework for nonlinear complex networks: An important-data-based method," *Int. J. Robust Nonlin. Control*, vol. 33, no. 4, pp. 2861–2878, Mar. 2023.
[38] H. Liu, Z. Wang, W. Fei, and J. Li, "Resilient $H_\infty$ state estimation for discrete-time stochastic delayed memristive neural networks: A dynamic event-triggered mechanism," *IEEE Trans. Cybern.*, vol. 52, no. 5, pp. 3333–3341, May 2022.
[39] S. Wen, Z. Zeng, and T. Huang, "Exponential stability analysis of memristor-based recurrent neural networks with time-varying delays," *Neurocomputing*, vol. 97, pp. 233–240, Nov. 2012.
[40] G. Zhang and Y. Shen, "Exponential stabilization of memristor-based chaotic neural networks with time-varying delays via intermittent control," *IEEE Trans. Neural Netw. Learn. Syst.*, vol. 26, no. 7, pp. 1431–1441, Jul. 2015.
[41] Y. Liu and L. Cheng, "Completely stealthy FDI attack against state estimation in networked control systems," *IEEE Trans. Circuits Syst. II, Exp. Briefs*, vol. 70, no. 3, pp. 1114–1118, Mar. 2023.
[42] P. Zhu, S. Jin, X. Bu, Z. Hou, and C. Yin, "Model-free adaptive control for a class of MIMO nonlinear cyberphysical systems under false data injection attacks," *IEEE Trans. Control Netw. Syst.*, vol. 10, no. 1, pp. 467–478, Mar. 2023.
[43] B. Wu, M. Chen, and L. Zhang, "Disturbance-observer-based sliding mode control for T-S fuzzy discrete-time systems with application to circuit system," *Fuzzy Sets Syst.*, vol. 374, pp. 138–151, Nov. 2019.
[44] J.-L. Chang, "Applying discrete-time proportional integral observers for state and disturbance estimations," *IEEE Trans. Autom. Control*, vol. 51, no. 5, pp. 814–818, May 2006.
[45] Y. Wang, L. Xie, and C. E. Souza, "Robust control of a class of uncertain nonlinear systems," *Syst. Control Lett.*, vol. 19, no. 2, pp. 139–149, 1992.
[46] L. El Ghaoui and G. Calafiore, "Robust filtering for discrete-time systems with bounded noise and parametric uncertainty," *IEEE Trans. Autom. Control*, vol. 46, no. 7, pp. 1084–1089, Jul. 2001.

**Lijuan Zha** received the Ph.D. degree in control science and engineering from Donghua University, Shanghai, China, in 2018.

She is currently an Associate Professor with the School of Science, Nanjing Forestry University, Nanjing, China, and also with the Nanjing University of Finance and Economics, Nanjing. She was also a Postdoctoral Research Associate with the School of Mathematics, Southeast University, Nanjing. Her current research interests include networked control systems, neural networks, and complex dynamical systems.

**Jinzhao Miao** received the B.S. degree in computer science and technology from the Nanjing University of Finance and Economics, Nanjing, China, in 2020, where he is currently pursuing the M.S. degree in computer science and technology with the College of Information Engineering.

His research interests include networked control systems, complex networks, and neural networks.

**Jinliang Liu** (Member, IEEE) received the Ph.D. degree in control theory and control engineering from the School of Information Science and Technology, Donghua University, Shanghai, China, in 2011.

He was a Postdoctoral Research Associate with the School of Automation, Southeast University, Nanjing, China, from December 2013 to June 2016. He was a Visiting Researcher/Scholar with the Department of Mechanical Engineering, University of Hong Kong, Hong Kong, from October 2016 to October 2017. He was a Visiting Scholar with the Department of Electrical Engineering, Yeungnam University, Gyeongsan, South Korea, from November 2017 to January 2018. From June 2011 to May 2023, he was an Associate Professor and then a Professor with the Nanjing University of Finance and Economics, Nanjing. In June 2023, he joined the Nanjing University of Information Science and Technology, Nanjing, where he is currently a Professor with the School of Computer Science. His research interests include networked control systems, complex dynamical networks, and time-delay systems.

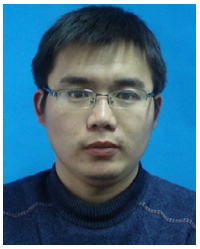

**Xiangpeng Xie** (Senior Member, IEEE) received the B.S. and Ph.D. degrees in engineering from Northeastern University, Shenyang, China, in 2004 and 2010, respectively.

From 2010 to 2014, he was a Senior Engineer with the Metallurgical Corporation of China Ltd., Beijing, China. He is currently a Professor with the Institute of Advanced Technology, Nanjing University of Posts and Telecommunications, Nanjing, China. His research interests include fuzzy modeling and control synthesis, state estimations, optimization in process industries, and intelligent optimization algorithms.

Prof. Xie serves as an Associate Editor for the *International Journal of Fuzzy Systems* and *International Journal of Control, Automation, and Systems*.

**Engang Tian** received the B.S. degree in mathematics from Shandong Normal University, Jinan, China, in 2002, the M.Sc. degree in operations research and cybernetics from Nanjing Normal University, Nanjing, China, in 2005, and the Ph.D. degree in control theory and control engineering from Donghua University, Shanghai, China, in 2008.

From 2011 to 2012, he was a Postdoctoral Research Fellow with the Hong Kong Polytechnic University, Hong Kong. From 2015 to 2016, he was a Visiting Scholar with the Department of Information Systems and Computing, Brunel University London, Uxbridge, U.K. From 2008 to 2018, he was an Associate Professor and then a Professor with the School of Electrical and Automation Engineering, Nanjing Normal University. In 2018, he was appointed as an Eastern Scholar by the Municipal Commission of Education, Shanghai, and joined the University of Shanghai for Science and Technology, Shanghai, where he is currently a Professor with the School of Optical-Electrical and Computer Engineering. He has published more than 100 papers in refereed international journals. His research interests include networked control systems, cyber attack, and nonlinear stochastic control and filtering.